MECSOL 2019 - Proceedings of the 7th International Symposium on Solid Mechanics
V. Tita, A. Ferreira, M.L. Ribeiro, A. Vieira and A.T. Beck (Editors), ABCM, Sao Carlos, SP, Brazil, April 15th to 17th, 2019

Optimization of thin-walled composite beams considering static loadings

Gabriel S. C. Souza[1], Éder Lima de Albuquere[2], G. B. Colherinhas[2], M. L. Ribeiro[1] and V. Tita[2]

[1] Aeronautical Engineering Department, São Carlos School of Engineering, University of São Paulo, Av. João Dagnone 1100, 13563-120 São Carlos, SP, Brazil
[2] Mechanical Engineering Department, Faculty of Technology, University of Brasília, Asa Norte, 70910-900 Brasília, DF, Brazil

Abstract. This work presents an evolutionary optimization method for single cell thin-walled composite beams based on a phenomenological failure criterion. A case study of a wing spar is described. The structural mechanical modeling developed considers axial warping and full anisotropic effects and does not include the influence of transverse shear loads. Using a genetic algorithm toolbox previously developed, some structural parameters are evaluated to reach optimal circular cross-section spar designs. Dimensional and structural project constraints are considered aiming a multi-objective fitness function that minimizes weight and maximizes the laminate stiffness. Comparisons between previously obtained results for the same structure are carried out.
Keywords: composite structures, thin-walled beams, optimization, genetic algorithms.

INTRODUCTION

The one-dimensional (1-D) modeling of thin-walled beams attracts the attention of several researchers since the work by Vlasov (1961). These models are applicable for structures made by isotropic materials with closed or open cross-sections. However, for beams composed of fibre reinforced composites the expansion of these models to anisotropic materials has to be carried out. In that manner, many researchers (Mansfield and Sobey, 1979; Kollar and Pluzsik, 2002; Librescu and Song, 2006; Zhang and Wang, 2014) dedicated works on developing models to describe the behavior of single/multicelled thin-walled composite beams (TWCBs) with open/closed cross-sections. These structures are used in many fields of engineering. For example, wind turbine blades are mostly manufactured of composite materials and those structures can be classified as TWCBs, e. g., if one dimension is compared to the others.

For practical optimization problems which aim a final product that satisfies its project's constraints in an optimal manner, the traditional 1-D beam model is preferred for a simplified modeling of these components due to the benefit of possessing a reduced number of degrees of freedom (Zhang and Wang, 2014). In this context, this work arises as a proposal to implement a one-dimensional theory formulated by Zhang and Wang (2014) for single cell thin-walled composite beams with arbitrary layup that accounts the effects of axial warping and full material anisotropy. Along with this, it is used a genetic algorithm (GA) toolbox developed by Colherinhas (2016) to optimize the wing spar of an unmanned aerial vehicle (UAV) under static loadings using the mechanical modeling approach and the failure criterion LaRC03 (Davila, Camanho and Rose, 2005).

THIN-WALLED COMPOSITE BEAMS: MECHANICAL MODELLING

Kinematics

Figure 1 presents a generic TWCB with constituent material some FRP composite laminate. Two coordinate systems are defined: global beam coordinate system OXYZ and local shell wall coordinate system nsz. Note that the angle θ is measured between the s-axis and the longitudinal fiber direction.

It is considered that the beam can be subjected to all sorts of loadings in all directions. In this context, there are made three kinematics hypotheses:

1. The cross-section plane of the beam behaves as a rigid body when subjected to loadings;
2. After experiencing rigid body movement, the cross-section remains perpendicular to its deformed normal axis;
3. Additionally to the rigid body movement of the cross-section, it is permitted that the beam has elastic axial warping.

Beam displacements in global coordinate system

There are six different rigid body movements of the beam cross-section: three translations and three rotations. These are the fundamental beam displacements. The translational displacements of a generic (X,Y,Z) point of the beam cross-

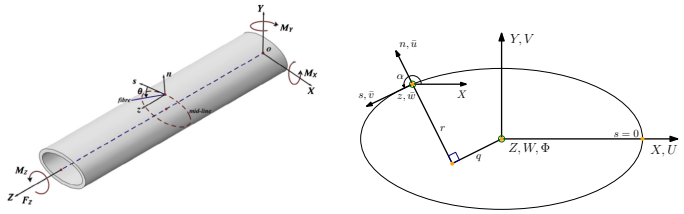

(a) (b)

Figure 1 – Definitions of global beam coordinate system and local shell wall coordinate system (a). Notations for sectional coordinates and displacements (b). (Zhang and Wang, 2014; Souza, 2017)

section is given by

$$\begin{aligned} U(X,Y,Z) &= U(Z) - \Phi_Z(Z)Y, \\ V(X,Y,Z) &= V(Z) + \Phi_Z(Z)X, \\ W(X,Y,Z) &= W(Z) + \Phi_X(Z)Y - \Phi_Y(Z)X, \end{aligned} \tag{1}$$

where the derivative is with respect to Z. Assuming that the effects of the shear strain can be neglected, it results that only one rotation is required to fully represent the beam movement. So, the angular displacement is given by $\Phi(Z) = \Phi_Z(Z)$. From the second hypothesis it follows that $U'(Z) = \Phi_Y(Z)$ and $V'(Z) = -\Phi_X(Z)$.

Local shell wall mid-surface displacements in local coordinate system

From the third hypothesis and the previous equations the displacements of a generic $(X(s), Y(s), Z)$ point of the beam cross-section is given by

$$\begin{aligned} U(X(s),Y(s),Z) &= U(Z) - \Phi(Z)Y(s), \\ V(X(s),Y(s),Z) &= V(Z) + \Phi(Z)X(s), \\ W(X(s),Y(s),Z) &= W(Z) + V'(Z)Y(s) - U'(Z)X(s) + \bar{w}_\omega(X(s),Y(s),Z), \end{aligned} \tag{2}$$

where $\bar{w}_\omega$ is the axial warping of the mid-surface. In contrast with the global displacements, it is worth noting that this quantity is locally described. Thus, the displacements of a point at the mid-surface at the local shell wall coordinate system are

$$\begin{aligned} \bar{u}(s,z) &= U(Z)\sin\alpha(s) - V(Z)\cos\alpha(s) - \Phi(z)q(s), \\ \bar{v}(s,z) &= U(Z)\cos\alpha(s) + V(Z)\sin\alpha(s) + \Phi(z)r(s), \\ \bar{w}(s,z) &= W(Z) - V'(Z)Y(s) -'(Z)X(s) + \bar{w}_\omega(s,z), \end{aligned} \tag{3}$$

where $r(s) = X(s)Y'(s) - Y(s)X'(s)$, $q(s) = X(s)X'(s) + Y(s)Y'(s)$, $\cos\alpha(s) = X'(s)$ and $\sin\alpha(s) = Y'(s)$.

Local shell wall generic point displacements in local coordinate system

Using the Kirchhoff-Love Plate Theory (Love, 1888), the displacements of a generic (n,s,z) point of the cross-section are

$$\begin{aligned} u(s,n,z) &= \bar{u}(s,z), \\ v(s,n,z) &= \bar{v}(s,z) - n\left[\frac{\partial\bar{u}(s,z)}{\partial s} - \frac{\bar{v}(s,z)}{R(s)}\right], \\ w(s,n,z) &= \bar{w}(s,z) - n\frac{\partial\bar{u}(s,z)}{\partial z}. \end{aligned} \tag{4}$$

Local shell wall generic point strains in local coordinate system

Using the strain-displacement relations from the Koiter-Sanders Shell Theory (Sanders, 1959; Koiter, 1967) in consistency with the Kirchhoff-Love Plate Theory the local strains of a generic point of the cross-section is given by

$$\begin{aligned}\varepsilon_{ss}(s,n,z) &= \bar{\varepsilon}_{ss} + n\bar{\kappa}_{ss},\\ \varepsilon_{zz}(s,n,z) &= \bar{\varepsilon}_{zz} + n\bar{\kappa}_{zz},\\ \gamma_{sz}(s,n,z) &= \bar{\gamma}_{sz} + n\bar{\kappa}_{sz},\end{aligned} \tag{5}$$

where $\bar{\varepsilon}_{ij}$ and $\bar{\kappa}_{ij}$ $(i,j = s,z)$ are the strains and curvatures of the mid-plane of shell wall, respectively. Here it will not be presented how to compute the local shell wall strains and curvatures of the mid-plane. The full demonstration can be found in the work by Zhang and Wang (2014).

Constitutive Equations of the Local Shell Wall in Local Coordinate System

For a generally orthotropic lamina it follows that the two-dimensional stress-strain relation in the local coordinate system is

$$\begin{Bmatrix}\sigma_{ss}\\ \sigma_{zz}\\ \sigma_{sz}\end{Bmatrix}_k = \begin{bmatrix}\bar{Q}_{ss} & \bar{Q}_{sz} & \bar{Q}_{sn}\\ \bar{Q}_{sz} & \bar{Q}_{zz} & \bar{Q}_{zn}\\ \bar{Q}_{sn} & \bar{Q}_{zn} & \bar{Q}_{nn}\end{bmatrix}_k \begin{Bmatrix}\varepsilon_{ss}\\ \varepsilon_{zz}\\ \gamma_{sz}\end{Bmatrix}_k . \tag{6}$$

Considering that $\bar{\kappa}_{ss} = 0$ and $\sigma_{ss} \approx 0$ (Zhang and Wang, 2014) it follows that the resultant of forces/moments-strain relation is given by

$$\begin{Bmatrix}N_{zz} & N_{sz} & M_{zz} & M_{sz}\end{Bmatrix}^T = \begin{bmatrix}k_{ij}\end{bmatrix}\begin{Bmatrix}\bar{\varepsilon}_{zz} & \bar{\gamma}_{sz} & \bar{\kappa}_{zz} & \bar{\kappa}_{sz}\end{Bmatrix}^T, \tag{7}$$

where k_{ij} is the stiffness matrix in the local coordinate system. Objecting to write the mid-plane shear strain and rearranging Eq. (7) it follows

$$\begin{Bmatrix}N_{zz} & M_{zz} & M_{sz} & \bar{\gamma}_{sz}\end{Bmatrix}^T = \begin{bmatrix}H_{ij}\end{bmatrix}\begin{Bmatrix}\bar{\varepsilon}_{zz} & \bar{\kappa}_{zz} & \bar{\kappa}_{sz} & N_{sz}\end{Bmatrix}^T, \tag{8}$$

where H_{ij} is the hybrid stiffness matrix. The name follows from the hybrid nature of the formulation using the Kirchhoff-Love Plate and Koiter-Sanders Shell theories. Note that now the shear strain is a function of the terms of the hybrid stiffness matrix, the axial strain and curvatures of the mid-plane where one can write $\bar{\gamma}_{sz} = H_{41}\bar{\varepsilon}_{zz} + H_{42}\bar{\kappa}_{zz} + H_{43}\bar{\kappa}_{sz} + H_{44}N_{sz}$. Thus, it considers the full anisotropic coupling that arises from the constituent material of the beam.

Constitutive Equations of the Beam in Global Coordinate System

The relation between the global forces and moments $F_Z, M_X, M_Y, M_\omega, M_Z$ applied to the beam and the global strains and curvatures $\in_Z, K_X, K_Y, K_\omega, K_{XY}$ is given by

$$\begin{Bmatrix}F_Z & M_X & M_Y & M_Z & M_\omega\end{Bmatrix}^T = \begin{bmatrix}E_{ij}\end{bmatrix}\begin{Bmatrix}\in_Z & K_X & K_Y & K_{XY} & K_\omega\end{Bmatrix}^T, \tag{9}$$

where E_{ij} is the global beam stiffness matrix and M_ω is the bimoment. In Eq. (9) K_X, K_Y are the global curvatures due to bending in the (X,Y) and (X,Z) planes, respectively; K_{XY} is the global twist rate of the beam; K_ω is the global curvature due to torsion of the beam. These are mathematically given by

$$\begin{aligned}&\in_Z = W'(Z),\ K_X = V'(Z),\\ &K_Y = -U''(Z),\ K_{XY} = \Phi'(Z),\\ &K_\omega = -\Phi''(Z).\end{aligned} \tag{10}$$

The methodology to compute the terms of the stiffnesses matrices k_{ij}, H_{ij} and E_{ij} can be found in the work by Zhang and Wang (2014).

DAMAGE MODEL: FAILURE CRITERION LARC03

In this work, it was used the failure criterion LaRC03 that distinguishes matrix and fiber failure modes, according to Davila, Camanho and Rose (2005). The criterion has a set of six distinct failure indexes (FI) to predict the structure collapse and there is no interaction one to another. This work does not aim to explore all the theory behind the formulation of LaRC03 so it limits itself by presenting it. More details about the failure criterion can be found in the work by Davila, Camanho and Rose (2005), who mentioned that is possible to identify the failure mode. However, the present authors believe that it is possible only to know how the homogenized ply fails under tensile or compression loadings in the direction 1 or 2.

According to Davila, Camanho and Rose (2005), from Tab. 1, it follows:

Table 1 – LaRC03 summary

Failure mode	Notation	Failure index
Matrix tension ($\sigma_{22} \geq 0$)	LaRC03 #2	$\text{FI}_M = (1-g)\frac{\sigma_{22}}{Y_{is}^T} + g\left(\frac{\sigma_{22}}{Y_{is}^T}\right)^2 + \left(\frac{\tau_{12}}{S_{is}^L}\right)^2$
Matrix compression ($\sigma_{22} < 0$)	LaRC03 #6	If $\sigma_{11} < Y^C$: $\text{FI}_M = \left(\frac{\tau_{\text{eff}}^{mT}}{S^T}\right)^2 + \left(\frac{\tau_{\text{eff}}^{mT}}{S_{is}^L}\right)^2$
	LaRC03 #1	If $\sigma_{11} \geq Y^C$: $\text{FI}_M = \left(\frac{\tau_{\text{eff}}^{T}}{S^T}\right)^2 + \left(\frac{\tau_{\text{eff}}^{L}}{S_{is}^L}\right)^2$
Fiber tension ($\sigma_{11} \geq 0$)	LaRC03 #3	$\text{FI}_F = \frac{\varepsilon_{11}}{\varepsilon_1^T}$
Fiber compression ($\sigma_{11} < 0$)	LaRC03 #4	If $\sigma_{22} < 0$: $\text{FI}_F = \left\langle \frac{\lvert\tau_{12}^m\rvert + \eta^L \sigma_{22}^m}{S_{is}^L} \right\rangle$
	LaRC03 #5	If $\sigma_{22}^m \geq 0$: $\text{FI}_F = (1-g)\left(\frac{\sigma_{22}^m}{Y_{is}^T}\right) + g\left(\frac{\sigma_{22}^m}{Y_{is}^T}\right)^2 + \left(\frac{\tau_{12}^m}{S_{is}^L}\right)^2$

If FIs are less or equal to "1" this implies that the ply does not fail. Notice that the safety factor is obtained by the relation $\text{SF} = 1/\text{FI}$.

OPTIMIZATION VIA GENETIC ALGORITHM

Genetic algorithms (GAs) were developed by Holland (1975) with the intention to mathematically describe the adaptation phenomenon that occurs in nature to implement it in computational systems. So, GAs are based on the mechanisms of natural selection, which presumes that the characteristics of the most adapted individuals with respect to some ambient pressure have the tendency of perpetuation through time. In that way, GAs try to mimic nature to search for the fittest solutions submitted to that environment pressure well defined by the programmer. Thus, populations of individuals (known as chromosomes) are randomly generated and evaluated by a fitness function that rank them according to one or more criteria. Then, those chromosomes are submitted to selection mechanisms and genetic operators such as cross-over and mutation to prosper through generations (Souza, 2017).

There are many strategies applied into those mechanisms that are widely documented in the literature (Colherinhas, 2016). The GA toolbox used in this work has real value codification to reduce computational cost during its execution and its implemented in MATLAB®. Moreover, it also makes use of uniform creep mutation that locally explores the search space by the hands of little perturbations on the genes randomly multiplying one of them by a value close to one and blend cross-over (BLX-α) which enlarges the father's crossing region rising genetic variability. Finally, elitism and decimation mechanisms, which are deterministic types of genetic operators, take role to preserve and remove those individuals with high and low values of fitness, respectively.

After the initial population being generated and its individuals evaluated by the fitness function, the algorithm has to select those which will pass to the next generation. Thus, a stochastic strategy is adopted by using the roulette-wheel method (Colherinhas, 2016; Souza, 2017). In that, an imaginary roulette will arbitrarily select the individuals based on the cumulative probability which is given by: $q_i = \sum_{k=1}^{i} P_k$, where P_k is the probability that an individual has of being chosen. The last is: $P_i = \frac{f(i)}{\sum_{i=1}^{N}}$, in which N is the number of chromosomes in the population.

Optimization Methodology

Figure 2 shows a flowchart to help the interpretation of the implemented functions in the GA toolbox.

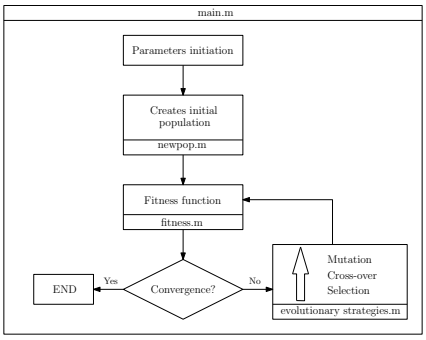

Figure 2 – Flowchart of the implemented functions (Colherinhas, 2016)

The *main.m* function is that which calls all the others. There occurs the parameters initiation, definition of the objectives and constraints' limits and the analysis of results (creation of the convergence graphics). The *fitness.m* receives the analytic formulations of the problem that one desires to solve and its output is the fitness value of the chromosomes. The generation of the initial population (based on the defined constraints' limits) is made by the *newpop.m* function while *evolutionary_strategies.m* executes the genetic operators in the defined order. Thus, at first, it applies the selection operator and, then, it processes with cross-over and mutation (each one with its own probability of occurrence). Table 2 shows the parameters used in the optimization process.

Table 2 – Optimization parameters

Parameter	Methodology	Value
Number of generations	-	200
Number of chromosomes per generation	-	200
Number of generations until next decimation	-	50
Decimation percentage	Deterministic	20%
Elitism percentage	Deterministic	2%
Mutation probability	Uniform creep	2%
Cross-over probability	BLX-α	60%

It is worth noting that those parameters were chosen after several tryout executions of the GA, and these are the ones that most attended the requisite of reducing computational cost without losing result quality.

Problem Description

The optimization proposal is to minimize the safety factor until the limit value of 1.5 with a tolerance of 0.05. Thus, spars with safety factor of 1.45 are taken as optimum ones due to this assumption. This is considered because the real span of the main spar is not equal the length of the wing, but it was considered for its design that these values are the same. So, here it will be assumed that this tolerance will result in a slightly conservative optimum solution which is good in terms of a preliminary design of the structure. The main objective here is to save time in the conceptual phase of the project, that is, the spar will pass through a refinement after this stage that implies to be analyzed in a Finite Element software and some experiments. As it is not the scope of this text, the methods to obtain the loadings acting on the spar during flight and landing are not discussed. These can be found in the work by Souza (2017).

Optimization Constraints

If no design constraints are defined, the GA will search for the solution in a much wider design space. In that way, it is necessary to well define constraints for any optimization problem. At this point one needs to decide which variables are going to be optimized. For this particular problem those are the medium radius (r_m), number of plies (N_p) and

fiber orientation (θ_i) each one limited by the following intervals: $16.2 \leq r_m \leq 19.4$mm, $2 \leq N_p \leq 5$ and $0^o \leq \theta_i \leq 90^o$, $i = 1,\ldots,N_i$.

For the medium radius, the limit is defined due to manufacturing limitations in the process and by the ribs' transverse thickness. The number of plies is defined such that the laminate possesses sufficient stiffness and does not weight too much and the angle limitation is trivial.

Fitness Function

It was decided to use 5^o and 15^o for maximum twist angle (Φ_i) restrictions for each critical condition (flight/landing), respectively. Thus, to fulfill this requirement, the fitness function maximizes the Failure Indexes (FI) of LaRC03 for matrix and fiber failure. As a consequence, that maximizes the safety factor. Considering only First Ply Failure (FPF) as design criterion, the fitness function (f_{obj}) is maximized by the following relation: $f_{\text{obj}} = \frac{1}{\text{fit}_i+1}$, with $i = 1,\ldots,N$, where $\text{fit}_i = |\min(\text{SF}_i) - \text{SF}_p|$, SF_p is the minimum project safety factor and i represents one chromosome of the population N. Note that this is a procedure to normalize the GA which makes the analysis easier. Thus, if $\min(\text{SF}_i) \rightarrow \text{SF}_p$, so $f_{\text{obj}} \rightarrow 1$. In that manner, the algorithm searches for solutions that possesses $\min(\text{SF}_i) \approx 1.5$ and that satisfies the restriction $\max\Phi_i \leq 5^o$ or 15^o for the twist angle. Finally, for those individuals that does not attend any of the previous criteria, it is defined $\text{fit}_i = 10$ resulting in low values for the fitness function. This was chosen after verifying that it provided good convergence characteristics for the GA.

RESULTS AND DISCUSSION

For the optimization, it is adopted a bidirectional (BD) carbon reinforced lamina with epoxy resin system. The thickness of the lamina is equal to 0.35 millimeters and its properties are shown in Tab. 3.

Table 3 – Carbon-epoxy BD reinforced lamina properties (Vasiliev and Morozov, 2013).

Properties	Value	Unit
Longitudinal Elasticity Modulus	70.0	GPa
Transverse Elasticity Modulus	70.0	GPa
Shear Modulus in the principal plane	5.8	GPa
Poisson's Ratio	0.09	-
Longitudinal Tensile Strength	860.0	MPa
Longitudinal Compressive Strength	560.0	MPa
Transverse Tensile Strength	850.0	MPa
Transverse Compressive Strength	560.0	MPa
Shear Strength in the principal plane	150.0	MPa

Optimization Results

Firstly, the optimization was divided in two separated problems for the critical flight and the landing conditions. After performing it several times for both cases, it comes that the flight condition is critical with respect to the stresses that are acting on the structure, implying in results with bigger medium radius. That means that spars found considering the critical flight condition resists the stresses produced by the critical landing condition. However, this does not mean that those structures attend the constraint of maximum torsional angle during landing. In that way, both optimization problems were united in a single one considering loadings from both critical conditions and the twist angle constraint becomes

$$\sqrt{(\max\Phi_i^L)^2 - (\max\Phi_i^F)^2} \leq \sqrt{15^2 - 5^2} = 14.142^o, \tag{11}$$

where $\max\Phi_i^L$ and $\max\Phi_i^F$ are the maximum twist angle of a chromosome i for landing and flight conditions, respectively. Equation (11) forces the GA to found solutions that stands the critical flight loadings and, at the same time, produces twist angles below the constraints for each condition under analysis. Considering only static loads, Fig. 3 shows the GA convergence curve. Table 4 shows the optimum values for the wing's main spar and exhibits the minimum SFs and the maximum twist angles for critical flight and landing conditions.

From Fig. 3 it can be noted that the fitness maximum value is not equal to "1". Thus, the minimum SF of the optimum solution differs from 1.5. Indeed, from Tab. 3 one can verify that its value is equal to 1.47. Though, that does not mean that

Table 4 – Optimum values, minimum SF and maximum twist angle for optimum spar

Parameter	Condition	Value	Unit
Mass	-	166.52	Grams
Medium radius	-	19.4	Millimeters
Number of plies	-	2	-
1st ply angle	-	65	Degrees
2nd ply angle	-	90	Degrees
Minimum Safety Factor	Flight	1.47	-
Maximum Twist Angle		2.36	Degrees
Minimum Safety Factor	Landing	2.69	-
Maximum Twist Angle		14.94	Degrees

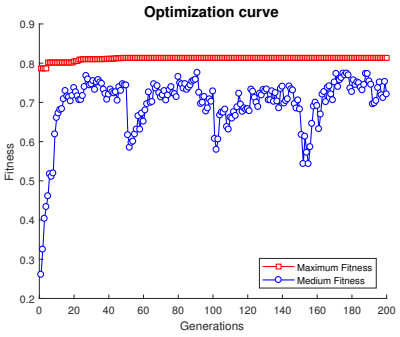

Figure 3 – Optimization convergence curve (fitness vs. generations)

the GA cannot lead to an optimum solution of the problem. In fact, the structure found by it is a result of considering the 0.05 tolerance in the minimum safety factor. Otherwise, it would not be capable of found a solution with only 2 plies for the laminate. That tolerance resulted from previous analysis considering the minimum SF equal to 1.5 which gave results with 3 plies. In that case, many spars could attend the constraints of maximum twist angle and minimum SF characterizing a *locus* of feasible solutions. In this context, the 0.05 tolerance was implemented to include the conservative assumption with respect to the length of the spar leading to a structure with only 2 plies, reducing mass of it and increasing structural efficiency.

Flight Condition

Figure 4 exhibits linear and angular displacements through the half span of optimum spar during the critical flight condition.

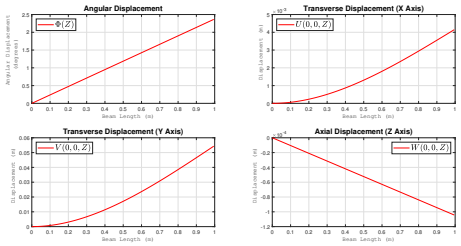

Figure 4 – Displacements of the optimum spar (critical flight condition)

From these graphics it is possible to notice the existence of an axial displacement due to the inherent coupling in the laminate. Besides that, the transverse displacements in the x and y directions produces maximum angles of 0.24^{o} and 3.12^{o}, respectively. Both values are not significantly at all for the design of the main wing spar because this condition of

bending is harmless to the performance of the aircraft if compared with twisting. It is worth noting that using the model developed by Zhang and Wang (2014) it was found values 8.19% lower for the transverse displacements in comparison with those found using the model by Librescu and Song (2006). For the twist angle the values are the same.

Figure 5 shows the local stress distribution at the longitudinal and transverse directions and the safety factor through the wall thickness at the critical cross-section for Tsai-Wu and LaRC03 failure criteria.

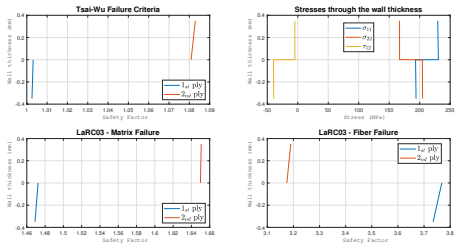

Figure 5 – Stresses and SF distributions through the wall thickness at the critical cross-section of the spar in the critical flight condition

Analyzing the stress distribution, it is clear that the failure modes of the fiber and matrix are due to transverse tension characterizing the use of LaRC03 #2 and #3 criteria, respectively. This means that the problem is found to be at the region of the failure envelope with most experimental data. The Tsai-Wu failure criterion provided more conservative results in comparison with the LaRC03. Another point is that the optimization using the first criterion would not lead to spars with 2 plies composing the laminate. Thus, it is notable the gain in structural efficiency using the LaRC03 failure criterion. This is, in part, a consequence of the usage of the *in-situ* strengths. When one analyzes an individual lamina of a laminate, its position in the stacking is relevant for its mechanical response. Here, it was considered that the laminae are thick in comparison with the crack's size (i.e. thick embedded plies). So, their *in-situ* transverse tensile and longitudinal shear strengths are constant and higher in comparison with their strengths when analyzed separately at the isolated lamina. Table 5 exhibits the parameters used for the LaRC03 failure evaluation.

Table 5 – LaRC03 parameters

Parameter	Symbol	Value	Unit
Fracture plane angle	α_0	53.0	Degrees
Toughness ratio	g	6.77	-
In-situ transverse tensile strength	Y_{is}^T	1362.2	MPa
In-situ longitudinal shear strength	S_{is}^L	212.1	MPa
Transverse shear strength	S^T	211.0	MPa
Transverse internal friction coefficient	η^T	0.287	-
Longitudinal internal friction coefficient	η^L	-0.288	-

Landing Conditions

Figure 6 shows the displacements of the spar during the critical landing case.

Similarly, it is verified a slight axial displacement on the beam. As in the previous case, this amount is harmless to the structure well-functioning. For the twist angle constraint, besides it is higher, attend the established restriction. The maximum transverse displacements in the x and y directions are -18.86 and 36.30 millimeters resulting in tip angles of 1.1^o and 2.1^o, respectively. The differences between the results of the models developed by Zhang and Wang (2014) and Librescu and Song (2006) are the same since the comparison is made for the same structure.

Figure 7 exhibits the local stress distribution at the longitudinal and transverse directions and the safety factor through the wall thickness at the critical cross-section for Tsai-Wu and LaRC03 failure criteria. Again, the failure modes are the same for fiber and matrix damage as in the critical flight condition. Also, the safety factors at the critical cross-section through the wall thickness of the spar are higher in comparison with the flight case. One interesting fact is that when using Tsai-Wu failure criterion the first ply would collapse while the second one is safe. For the flight case, both plies are safe from failure. Additionally, notice that for the first ply lowers safety factors are found at the critical cross-section for the

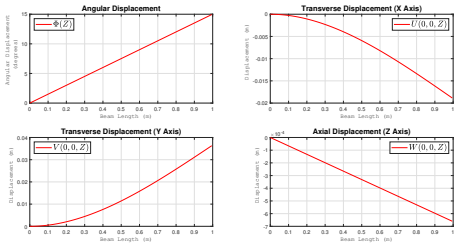

Figure 6 – Displacements of the optimum spar (critical landing condition)

landing condition when compared to the same ply for the flight condition when using Tsai-Wu criterion. Indeed, it can be verified that the normal stresses are lower while shear stresses are higher. Thus, the Tsai-Wu failure criterion can be much sensitive to shear stresses (when those possesses magnitude similar to normal stresses) near the longitudinal shear strength in the case of laminae with bidirectional reinforcement.

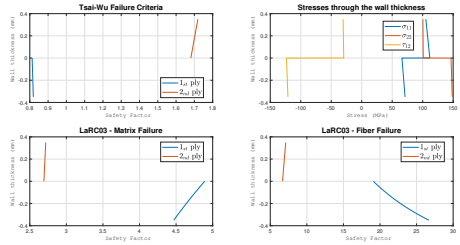

Figure 7 – Stresses and SF distributions through the wall thickness at the critical cross-section of the spar in the critical landing condition

CONCLUSIONS

In this study, the optimization problem of a beam composed of fiber reinforced polymer composite material was assessed allying the usage of LaRC03 failure criterion and the mechanical modelling for thin-walled composite beams developed by Zhang and Wang (2014). Comparisons between LaRC03 and Tsai-Wu failure criteria and the models by Zhang and Wang (2014)/Librescu and Song (2006) were made. The optimization was realized through the GA toolbox developed by Colherinhas (2016). Although it was applied in a particular way, this methodology can also be used in many other kinds of problems, e. g., wind turbine blades. In this context, some conclusions can be done.

Firstly, the model by Zhang and Wang brings significantly improvements in contrast with the one of Librescu and Song. The last model does not consider the intrinsic anisotropies inherent to composite materials with regard to the computation of the mid-plane shear strain $\bar{\gamma}_{sz}$ while the first, doing it directly from the constitutive equation, is capable of obtaining with more precision the beam mechanical response. In fact, it can be verified that the discrepancy between these models can reach more than 60% in the computation of the bending stiffness for the same laminate (Zhang and Wang, 2014; Souza, 2017).

In reference to the failure criteria contrasted, the LaRC03 is more capable of predicting first ply damage mainly for fiber or matrix failure under compression. Also, this criterion is capable of capturing the *in-situ* effects inherent to laminate failure analysis and requires only two additional experiments for its characterization in contrast with the Tsai-Wu criterion. For the specific problem studied, the usage of LaRC03 criterion provided a less conservative structure. This possesses [65/90] stacking sequence, medium radius of 19.4 millimeters and final mass of 166.52 grams. This means that the GA achieved an asymmetric laminate. If, for the same problem, is used this methodology allied with Tsai-Wu criterion one would find a structure with same medium radius but with three plies in the stacking sequence implying in a final mass of 249.78 grams. That means an increase of 33% in the mass of the beam, reducing significantly the structural efficiency of it. The same structure previously designed using Tsai-Wu failure criterion and the Classical Laminate Theory has [0/0/0] stacking sequence. Similarly results using genetic algorithms for the optimization of the stacking sequence of a laminate were found by Almeida et. al. (2017). In that work, the optimization of composite tubes under internal pressure

accounting for progressive damage was assessed. The results obtained shows that progressive failure analysis generates asymmetric and unbalanced laminates supporting the results presented in the present work.

CONSIDERATIONS AND FUTURE WORKS

Until the present moment, the algorithm shows consistent results for static loadings. Based on the preliminary results, it was obtained a mass reduction of 33%. For the future works, the mechanical modelling can be extended to account for shear strain due to transverse shear loadings, geometrical non-linearities due to large deformations and variable cross-section through the beam's length. Moreover, a study can be conducted to consider tapered laminates in the optimization problem.

For the GA toolbox, it is suggested that the routines are wrote in another language such as Python, Fortran or C. In the case of studying problems with greater degree of complexity this is a way to reduce computational cost. To know, the present algorithm takes approximately 35 minutes to generate results in a notebook Intel Core i7-4500U, 2.4 GHz, 8GB of RAM (DDR3) and Windows 10 operational system.

Finally, it is important the study of progressive failure to contrast optimum individuals found by using First Ply Failure and Last Ply Failure approaches.

ACKNOWLEDGEMENTS

The authors acknowledge the financial support of the National Council for Scientific and Technological Development and Coordination for the Improvement of Higher Education Personnel. Gabriel S. C. Souza acknowledges Draco Volans team from University of Brasília for the data provided.

REFERENCES

Almeida, J. H. S. et. al. "Stacking sequence optimization in composite tubes under internal pressure based on genetic algorithm accounting for progressive damage", Composite Structures, Vol. 178, pp. 20-26, 2017.

Colherinhas, G. B. "Ferramenta de otimização via algorítmos genéticos com aplicações em engenharia", Master's Thesis, University of Brasília, 2016.

Davila, C. G.; Camanho, P. P. and Rose, C. A. "Failure criteria for FRP laminates", Journal of Composite Materials, Vol. 39, n. 04, pp. 323-345, 2005.

Holland, J. H. "Adaptation in natural and artificial systems: an introductory analysis with applications to biology, control and artificial intelligence", University of Michigan Press, Oxford, 1975.

Koiter, W. T. "General equations of elasticity stability for thin shells", Proceedings of the University of Houston – Symposium on Theory of Shells, pp. 185-227, 1967.

Kollar, L. P. and Pluzsik, A. "Analysis of thin-walled composite beams with arbitrary layup", Journal of reinforced plastics and composites, Sage Publications, Vol. 21, n. 16, pp. 1423-1465, 2002.

Librescu, L. and Song, O. "Thin-walled composite beams. Theory and application", Solid Mechanics and It's Applications, Springer, Vol. 131, 1st ed., 2006.

Love, A. E. H. "The small free vibrations and deformation of thin elastic shell", Philosophical Transactions of the Royal Society of London, Vol. 179, pp. 491-546, 1888.

Mansfield, E. and Sobey, A. "The fibre composite helicopter blade", Aeronautical Quarterly, Cambridge University Press, Vol. 30, n. 02, pp. 413-449, 1979.

Sanders, J. J. L. "An improved first-approximation theory for thin shells", NASA Technical Reports, n. R-24, 1959.

Souza, G. S. C. "Otimização genética de vigas de paredes finas compósitas: uma abordagem fenomenológica", Bachelor Thesis, University of Brasília, 2017.

Vasiliev, V. and Morozov, E. "Advanced mechanics of composite materials", Elsevier, 3rd ed., 2013.

Vlasov, V. Z. "Thin-walled elastic beams", Israel Program for Scientific Translations, 2nd ed., 1961.

Zhang, C. and Wang, S. "Structure mechanical modeling of thin-walled closed-section composite beams, part 1: Single-cell cross section", Composite Structures, Vol. 113, pp. 12-22, 2014.

RESPONSIBILITY NOTICE

The authors are the only responsible for the printed material included in this paper.